Proc. 2010 IEEE International Ultrasonics Symposium, San Diego, CA, Oct. 11-14, 2010, pp. 543-546

Anomalous dispersion of SAW in platinum grating on langasite with Euler angles (0º, 138.5º, 26.6º)

Natalya Naumenko
Moscow Steel and Alloys Institute, Moscow, Russia
nnaumenko@ieee.org

***Abstract* — The numerical technique recently developed for simulation of SAW dispersion in periodic gratings was applied to langasite cut with Euler angles (0º,138.5º,26.6º) and platinum grating, when electrode thickness varies between 1% and 6% λ (SAW wavelength). Analysis has revealed that with increasing Pt thickness, the dispersion appears to be strongly affected by interaction between two SAW modes. It results in additional stopband, which occurs at certain detuning from synchronous reflection condition and manifests itself by additional resonances of admittance function if such detuning occurs in SAW resonator. The anomalous character of dispersion is not adequately described by the known COM models and can explain the slow growth of reflectivity with increasing electrode thickness.**

I. Introduction

In the last two decades, utilizing of passive surface acoustic wave (SAW) devices for the development of wireless sensor systems has aroused an increasing interest [1]. Temperature sensors with resonator-type structure operating in a wide range of temperatures, up to 700ºC, can be built on langasite, $La_3Ga_5SiO_{14}$ (LGS). This crystal provides a successful combination of low acoustic propagation losses, sufficiently high electromechanical coupling factor and ability to work at high temperatures, due to high melting point and absence of phase transitions. The temperature compensated orientation with Euler angles (0º, 138.5º, 26.6º), which was originally found as the optimal cut for SAW filters [2], can be also implemented in wireless temperature SAW sensors, due to acceptable value of maximum frequency shift within wide range of temperatures. As electrode material, platinum (Pt) is the best choice, because of its low resistivity at high temperatures and good adhesiveness of metallic layer to the substrate [3].

To predict the behavior of SAW resonator on LGS substrate, coupling-of-mode (COM) model is commonly exploited. This assumes that one of two known dispersion equations, which describe either perfect Rayleigh SAW [4] or SH-type SAW [5], adequately characterizes the behavior of surface wave in a periodic grating and only parameters of this equation need to be determined. The present work is aimed at investigation of the behavior of SAW in platinum grating on langasite cut mentioned above, in order to answer the question, which of two known COM equations better characterizes SAW dispersion and should be used for simulation of SAW resonators on LGS.

II. Method of Analysis

The recently developed numerical technique using "rational approximation" of harmonic admittance [6] enables fast and accurate calculation of dispersion in arbitrary orientation, independent on the type of SAW propagating in it. Moreover, if two SAW modes exist in the analyzed orientation, the interaction between them is automatically taken into account and its effect on SAW dispersion can be simulated. This method was applied to LGS cut with Euler angles (0º, 138.5º, 26.6º) and Pt grating of thickness varying between 1% λ and 6% λ, where λ=2p is SAW wavelength at Bragg reflection condition and p is a period of the grating. The results of calculations are discussed below. All calculations were performed with constants reported in [7].

III. Results of Calculations and Discussion

One of the most important characteristics of SAW resonator is reflection coefficient per period of the grating or per wavelength, κ. For fixed combination of a substrate and electrode materials, this and other parameters depend on electrode thickness and geometry. In non-symmetric cuts, an example of which is the analyzed LGS orientation, κ is complex and its amplitude and phase can be estimated from two resonances and two anti-resonances, which occur at both edges of the reflection stopband, for short-circuit (SC) and open-circuit (OC) electrical conditions, respectively.

Two mechanisms contribute the reflection coefficient: piezoelectric coupling of SAW with applied voltage and mass load of electrodes. One can expect that for heavy electrode material, such as Pt, abs(κ) must be much higher than for aluminum (Al) electrodes of the same thickness, because Al has nearly 8 times lower mass density. Fig. 1a, b shows the calculated electromechanical coupling factor k^2 and reflection coefficient per wavelength κ in (0º, 138.5º, 26.6º)-LGS with Pt and Al gratings, as functions of electrode thickness h/λ. The coupling k^2 grows with electrode thickness much faster for Pt grating, but the behavior of κ does not agree with expected. At

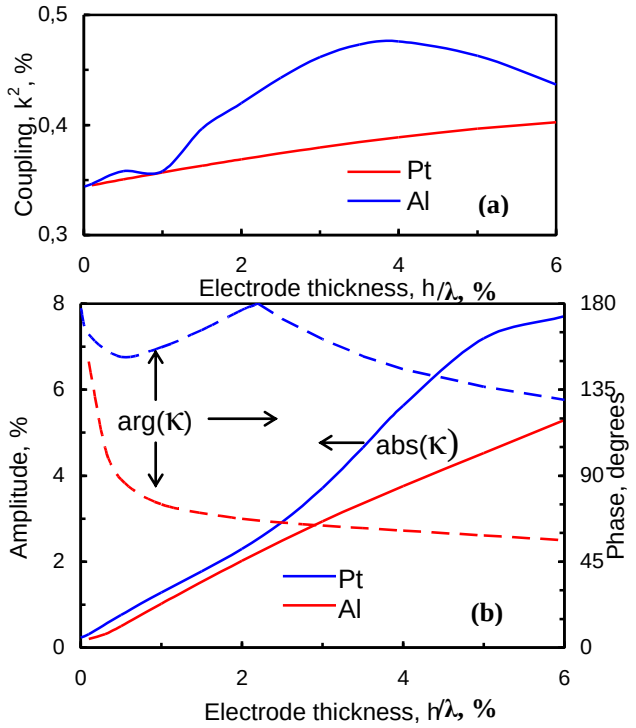

Fig.1. Characteristics of SAW in LGS with Pt grating, as functions of electrode thickness: electromechanical coupling (a) and reflection coefficient per wavelength (b). The module and phase of reflection coefficient for Pt grating (blue lines) are compared with that of Al grating (red lines).

h<2.5%λ its absolute value for Pt is nearly the same as for Al, and when h>2.5%λ, though abs(κ) grows faster for Pt electrodes, it is not as high as expected. The behavior of arg(κ) looks different for two metals.

To understand the reasons of low reflectivity in Pt grating, first all resonant frequencies were extracted from admittance Y(f) as functions of Pt thickness. The results are shown in Fig.2 and reveal the existence of the 3-rd resonance, in addition to two resonances at the edges of the stopband. This third resonance apparently refers to another mode (SAW2) propagating in the same orientation with higher velocity. It arises from BAW at about h_{Pt}≈0.5% λ and the velocity dependences of two modes look as nearly parallel lines. The interaction between two modes can be understood from the dispersion plots. Fig.3a, Fig.4a and Fig.5a demonstrate velocity dispersion in the grating calculated at three different Pt thicknesses, 1%, 2% and 4%λ, respectively.

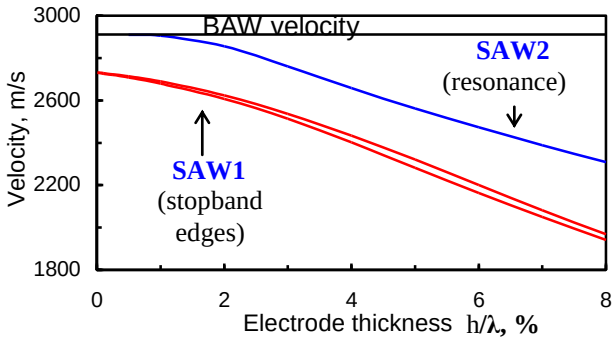

Fig.2. Velocities of two SAW modes propagating in LGS with Pt grating estimated at resonant frequencies, as functions of normalized electrode thickness

For small Pt thickness (Fig.3), four modes propagating in the grating can be seen clearly: two forward modes (n=0) and two backward modes (n=−1). They refer to SAW1 and BAW. The coupling between the counter propagating SAW1 modes builds the stopband at f′=0.460-0.461, where f′=fp/V_{BAW} is the normalized frequency. Another stopband arises from SAW1/BAW interaction, which starts at the cut-off frequency, f′≈0.478, and manifests itself by increasing BAW radiation, Im(V)>0, when f′>0.478. The third stopband occurs at f′≈0.499 and can be referred to the coupling between counter propagating SAW2 modes, with velocities and wave structure very close to that of the bulk wave.

The edges of the lower stopband (SAW1) and the lower edge of the upper stopband (SAW2) manifest themselves as three resonances of admittance Y(f) calculated at synchronous resonance condition, λ=2p (Fig.3b), at f_{R1}=0.46, f_{R2}=0.461 and f_{R3}=0.499. SAW/BAW interaction at f′≈0.478 does not produce noticeable perturbation of the admittance function.

With Pt thickness 2%λ (Fig.4), the following stopbands are built by interactions between two SAW modes:

1) f′=0.447-450 - SAW1/SAW1 interaction;
2) f′=0.464-474 - SAW1/SAW2 interaction;
3) f′>0.490 - SAW2/SAW2 interaction.

For the first interaction, the phase of reflection coefficient is close to 180º. Therefore, there are only two resonances, at f′=0.447 and f′=0.490 and no resonance at f′=0.450, if the admittance is calculated at λ=2p. The second stopband occurs at certain detuning from this synchronous condition, Δs=p/λ-s_0, where s_0=0.5, which slowly varies within the stopband. For example, the admittance calculated at Δs/s_0=5.3% reveals strong resonance at f′=0.464.

With further increasing Pt thickness, the second and third stopbands (SAW1/SAW2 and SAW2/SAW2 interactions) merge and at h_{Pt}=4%λ (Fig.5) they produce very wide *detuned* stopband, f′=0.420-0.453, with normalized detuning parameter decreasing within this interval from Δs/s_0=5.4% to zero. It is located close to SAW1/SAW1 stopband, (f′=0.409-417), and adds one resonance to admittance, at f′=0.453, if Δs=0. If proper detuning is fixed, another resonance appears at the lower stopband edge, f′=0.420, as shown in Fig.5b.

The close proximity of two stopbands apparently means that the reflection of SAW1 in the grating is dramatically affected by interaction between SAW1 and SAW2. Moreover, the coupling between two SAW modes looks stronger than SAW1/SAW1 coupling. Such anomalous dispersion cannot be described by any of two known COM models.

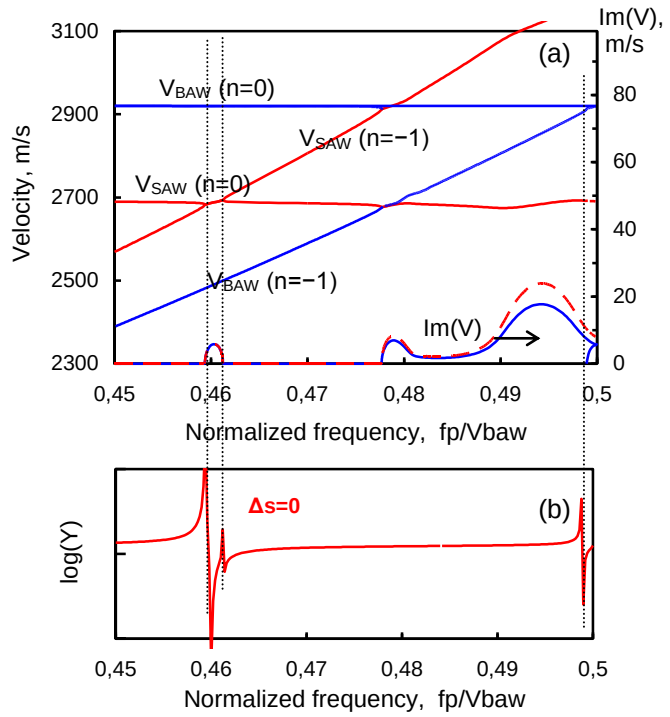

Fig.3. Velocity dispersion in SC grating (a) and harmonic admittance calculated at synchronous resonance condition (b), in Pt grating on LGS, when electrode thickness is h=1%λ

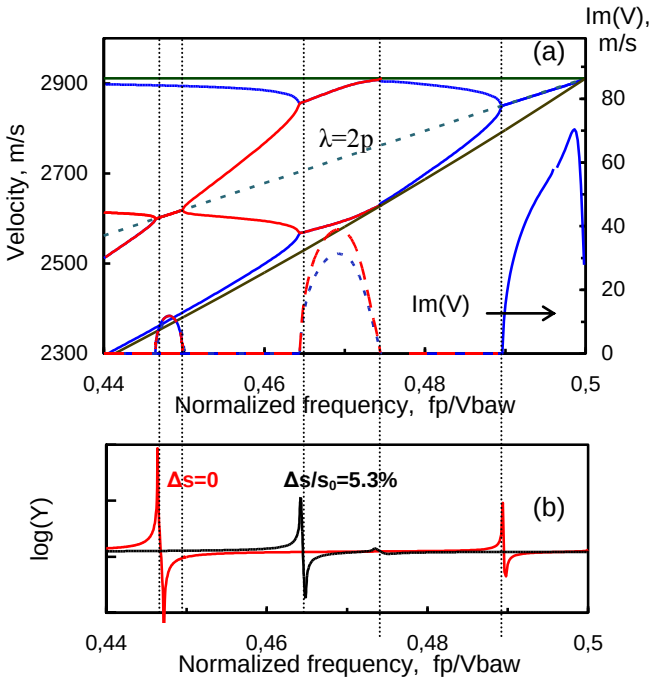

Fig.4. Velocity dispersion in SC grating (a) and harmonic admittance calculated at synchronous resonance (b), λ=2p and at certain detuning, in Pt grating on LGS, when electrode thickness is h=2%λ

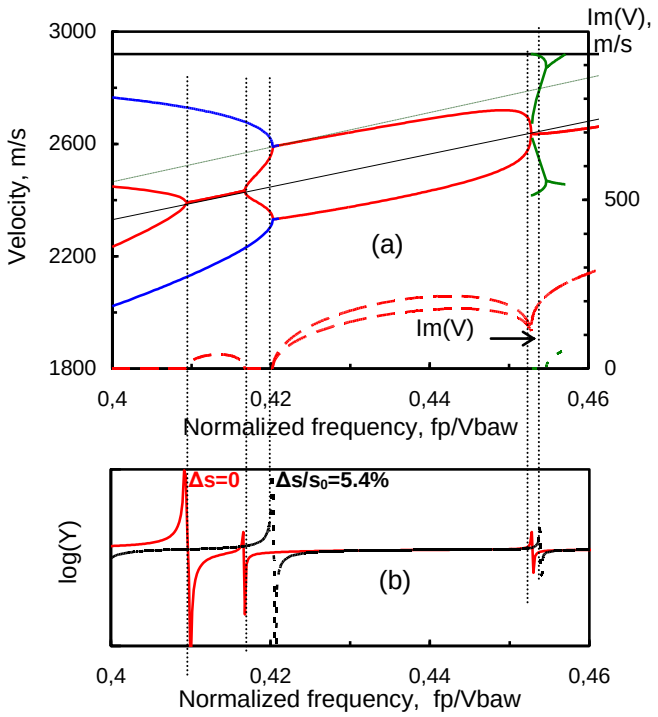

Fig.5. Velocity dispersion in SC grating (a) and harmonic admittance calculated at λ=2p and at certain detuning (b), in Pt grating on LGS, when electrode thickness is h=4%λ

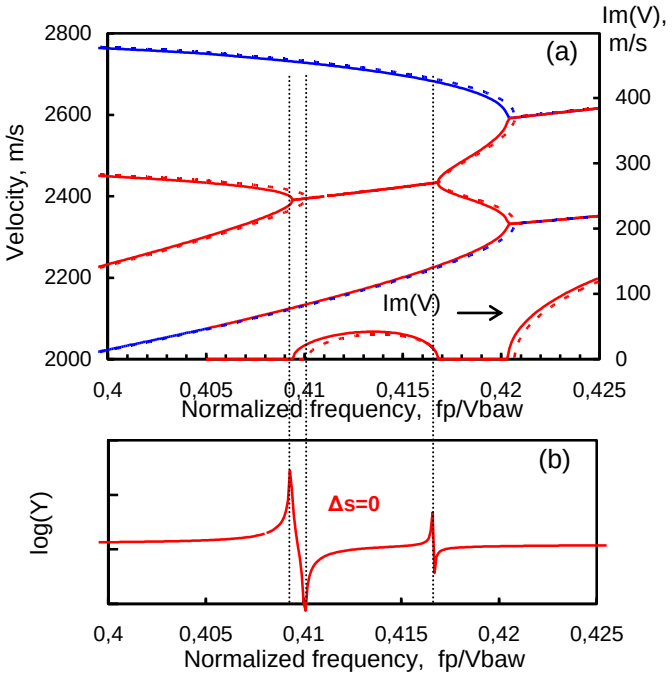

Fig.6. Velocity dispersion in SC and OC gratings (a) and harmonic admittance calculated at synchronous resonance condition (b), in Pt grating on LGS, when electrode thickness is h=4%λ

Fig.6 demonstrates the enlarged fragment of Fig. 5, with calculated velocity dispersion at h_{Pt}=4%λ, in SC and OC gratings. The shift between the stopband edges obtained for different electrical conditions means the natural unidirectivity of SAW propagation, which is typical for non-symmetric orientations and results in the phase of reflection coefficient non-equal zero or 180º.

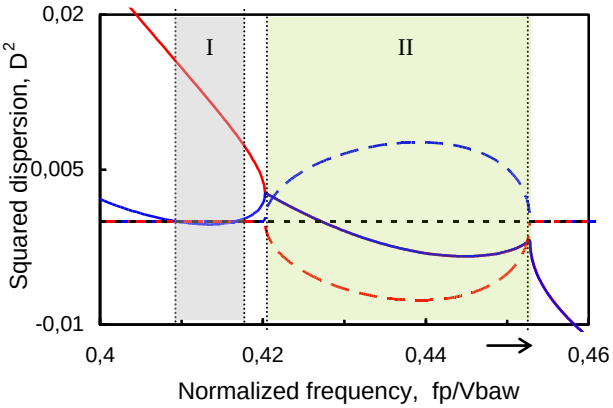

Fig.7. Real (solid lines) and imaginary (dashed lines) parts of dispersion parameter $D^2=(\Delta s/s_0)^2$, as functions of normalized frequency, in SC grating with Pt electrodes on LGS, h=4%λ. Two stopbands refer to interactions between counter propagating SAW1 (shaded area I) and counter propagating SAW1 and SAW2 (area II).

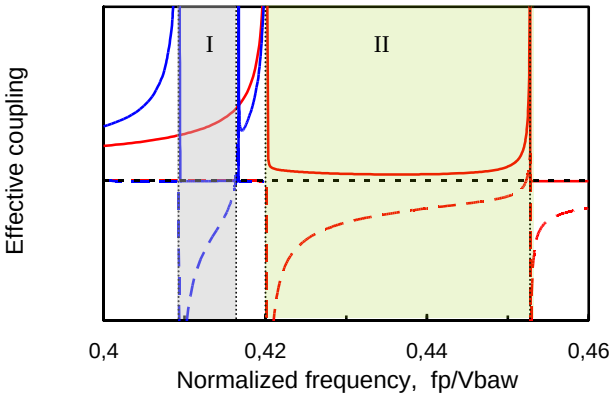

Fig.8. Real (solid lines) and imaginary (dashed lines) parts of effective coupling coefficient K_{eff}, as functions of normalized frequency, in SC grating with Pt electrodes on LGS, h=4%λ.

Fig.7 gives another interpretation of the results shown in Fig.5. The squared dispersion parameter $D^2=(\Delta s_R/s_0)^2$ is shown for two grating modes, as function of normalized frequency, where Δs_R satisfies the SC electrical condition $Y(f,\Delta s_R)^{-1}=0$. This parameter represents the energy storage in the grating. Two shaded areas indicate the stopbands built by SAW1/SAW1 (area I) and SAW1/SAW2 (area II) interactions.

In the area I, two perturbed SAW modes have wave numbers $s_{1,2}=(0.5\pm\Delta s_R)$ with pure imaginary Δs_R. Hence, Δs_R^2 is real. In the area II, the result of interactions between SAW1 and SAW2 are four modes with perturbed wave numbers, $s_{1,2,3,4}= (0.5\pm\Delta_{RE}\pm j\Delta_{Im})$, where Δ_{RE} and Δ_{Im} are pure real and the squared dispersion parameter is complex, $\Delta s_R^2=(\Delta_{RE}^2-\Delta_{Im}^2) \pm 2j\Delta_{Re}\Delta_{Im}$, i.e. two pairs of wave solutions have complex conjugate parameters Δs_R^2, as shown in Fig. 7.

Another important parameter, which characterizes frequency dependent excitation in the grating is shown in Fig.8. It is effective piezoelectric coupling factor. In the area II (second stopband), its behavior differs from that typical for SAW: inside this frequency interval, the coupling is complex.

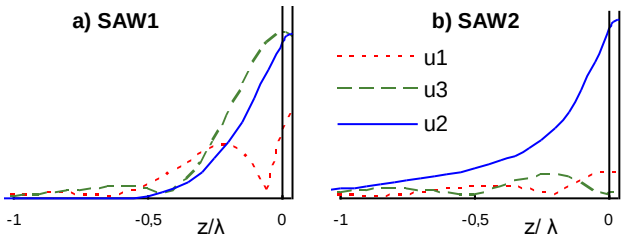

Fig.9. Displacements along vertical axis, in LGS with Pt grating (SC), h_{Pt}=4%λ, calculated at normalized frequency f'=0.4: (a) SAW1, (b) SAW2.

Besides, strong radiation is expected at the edges of the second stopband.

The nature of two SAW modes propagating in the analyzed cut is illustrated in Fig.9, which shows the amplitudes of displacement components of SAW1 and SAW2 propagating in SC grating with Pt thickness 4%λ, at the normalized frequency f'=0.4, for which both modes stay unperturbed. SAW2 is more close to SH-type wave, while SAW1 looks as generalized SAW with ellipse of polarization rotated around X-axis of the substrate.

IV. Conclusions

In langasite cut with Euler angles (0º, 138.5º, 26,6º) and Pt grating, interaction between two SAW modes occurs and results in anomalous dispersion of SAW in the grating. This dispersion is not adequately described by any of two known dispersion equations. For accurate simulation of SAW resonators, the frequency-dependent COM parameters should be used if the thickness of platinum grating exceeds 2% of SAW wavelengths.

References

[1] S. Ballandras, W. Daniau, G. Martin, and P. Berthelot, "Wireless Temperature Sensor using SAW Resonators for Immersed and Biological Applications", in *Proc. IEEE Ultrason. Symp.* pp. 445-448, 2002.

[2] N.F.Naumenko, and L.P.Solie, "Optimal cut of langasite $La_3Ga_5SiO_{14}$ for SAW devices", *IEEE Trans. Ultrason. Ferroelectr. Freq. Contr.*, vol.48, no 2, pp.530-537, 2001.

[3] J.A. Thiele, and M. Pereira da Cunha, "Platinum and Palladium High-Temperature Transducers on Langasite", *IEEE Trans. Ultrason. Ferroelectr. Freq. Contr.*, vol. 52, no. 4, pp. 545-549, 2005.

[4] K. Blǿtekjær, K. Ingebrigtsen, and H. Skeie, "Acoustic Surface Waves in Piezoelectric Materials with Periodic Metal Strips on the Surface", *IEEE Trans. Electron. Devices*, vol. 20, pp.1139-1146, 1973.

[5] V. P. Plessky, "Two parameter coupling-of-modes model for shear horizontal type SAW propagating in periodic gratings", in *Proc. IEEE Ultrason. Symp.*, pp. 195-200, 1993.

[6] N. Naumenko, and B. Abbott, "Fast numerical technique for simulation of SAW dispersion in periodic gratings and its application to some SAW materials", in *Proc. IEEE Ultrason. Symp.* pp.166-170, 2007.

[7] A. Bungo, C. Jian, K. Yamaguchi, Y. Sawada, R. Kimura, S. Uda, "Experimental and theoretical analysis of SAW properties of the Langasite Substrate with Euler Angle (0°,140°,θ), in *Proc. IEEE Ultrasonics Symp.*, pp 231-234, 1999.